Studies on Compression Behavior of Carbon–Epoxy Laminates With and Without Buffer-Strip Layers in Dry and Water-Absorbed Conditions

KISHORE,[1] BIJOYSRI KHAN,[1] B. VISWANATH[2]

[1] Polymer Composites Laboratory, Department of Metallurgy, Indian Institute of Science, Bangalore 560 012, India

[2] Composite Structures Division, Aeronautical Development Establishment, Bangalore 560 075, India

Received 11 January 2001; accepted 19 March 2001

ABSTRACT: This work looks at the compression behavior of laminated carbon–epoxy (C–E) composites with inserted interleaved polytetrafluoroethylene-coated fabric material at different locations either continuously or discontinuously within the specimen. Also, the effect of water ingress in these specimens on the strength values is reported. Although significant differences were noticed in the trend of the strengths for different architectural arrangements in dry and water-immersed samples, significant differences for the modulus was less perceptible. The introduction of small amounts of less-adherent layers of material at specific locations causes a decrement in the load-carrying capability of the C–E system. It is further observed that with an increase in the number of buffer/delaminating strips insertions, the water ingress increases and the compressive strength values decrease. Examination of the samples, noting macroscopic features including the interfacial regions, assisted in observing a correlation between the observed strength values, architecture, and the failure mode. © 2002 John Wiley & Sons, Inc. J Appl Polym Sci 83: 408–416, 2002

Key words: interleaved structures; impact behavior; interface; delamination; damage tolerance

INTRODUCTION

Composite materials are being used extensively in aerospace and other technologically advanced applications. Concentrated efforts are under way in many laboratories to further improve upon its performance. Thus, modification of the matrix, inclusion of particulate/fillers, surface treatment of reinforcement to enhance adhesion,[1] hybridization of reinforcement structure, sandwiching foam core with strong facing materials, and so on have made the perusal of composite literature exciting and invite the attention of materials scientists and engineers alike. An area that has caught significant attention is one involving improvement upon the impact resistance of the composites.[2,3] In this context, the use of tough (elastomeric) materials is cited.[4] Although toughness does get enhanced in neat polymers, that for the case of reinforced ones, the improvements are comparatively less spectacular. This is an area that needs serious investigation.

Another way to look at the problem of improving the performance of the composites is to study its performance with deliberately inserted interleaved material. With such insertions, the response to impact changes.[5,6] Apart from characterizing the dynamic response, there is a great

Correspondence to: Kishore (balkis@metalrg.iisc.ernet.in).

Journal of Applied Polymer Science, Vol. 83, 408–416 (2002)

need to study the static response[7] in general and compression[8–10] in particular, as often structural members are subjected to compressive loading situations. The present effort addresses this issue in carbon–epoxy (C–E) with polytetrafluoroethylene (PTFE)-coated buffer strip inserted interleaved material that is arranged continuously in one case and discontinuously in the other. In the latter case, this work looks at how the performance of the material would be when the strips are positioned closer to the loading platen in one case and away from it in the other. Also, because the less adhering strip would be a potential site for temporary sinks for the water-ingressed molecules, how the differently architectured (i.e., strip bearing) samples perform in compressive loading following a stipulated time immersed in water is also examined in this work. This ingress, especially along weakly adhering strips and consequent absorption of water by the system leading to volumetric expansion, can cause an overall structural change that is both challenging and complex. The approach adopted in the present case, therefore, involves conducting static tests on dry and water-ingressed C–E samples with and without either discontinuously or continuously posited buffer strips. The load-deflection data derived are used to deduce the values of compression strength and elastic modulus. As the architecture of the samples varied and further water immersion added a new dimension to the structural features within the samples, it was decided to correlate the strength data with macroscopic features exhibited by test coupons following compression. This kind of structure–property correlation is infrequently reported in composite materials in general and C–E systems in particular and hence is addressed in this work.

EXPERIMENTAL

Laminates were made by using C–E prepreg (supplied by Ciba-Geigy) stacks of 16 layers to yield specimens of 5 mm thickness. Strips of PTFE-coated fabric with a width of 5 mm and a thickness of 0.02 mm were introduced at different positions and layers of the lay-up. These strip materials were selected, because they are prone to debonding about the interfacial regions comprising the strip material and C–E system. The buffer/delaminating strips (BS) were used either in continuous form running through the length or in a discontinuous way occupying select regions during the stacking sequence. The woven PTFE-coated fabric (due to its meshlike openings) allowed for the resin to establish contact with the adjoining resin matrix regions. The region constituted by the immediate environs of the PTFE-coated fibers of the BS fabric themselves, on the other hand, corresponds to areas of less adhesion due to the inherent poor-bonding nature associated with this kind of coated material. How this localized change in structural detail due to incorporation of interleaf material, with different interface adhesion characteristics, affects the compressive load carrying capability forms a principal aim of this investigation. To achieve a gradation in structural change, in the first category, C–E samples alone were made. These were termed plain and given a code of 0, because it had no PTFE-coated buffer strips inserted within them. In making the next category, the BS was introduced in the mid plane and given a code with a starting number of 1 because only one layer region containing the BS was inserted. For the third variety, BS was introduced at two places, namely, about one-third and two-third layer (i.e., along the thickness) positions, and these were coded with a starting number of 2. In fabricating the fourth and last category laminates, the BS was introduced at three specific places, namely, one-fourth, one-half, and three-fourth layer (again along the thickness) positions. These samples, following the coding employed, were designated with a starting number of 3.

The above three categories of BS-bearing specimens (i.e., series starting with 1, 2, and 3) were further subclassified depending on whether the BS were in the form of continuous or discontinuous strips. That is, (i) continuous delaminating strip [CT Fig.1(a)]; and (ii) discontinuous delaminating strips (D). In these latter specimens, the strips were discretely distributed through the length, and by its basic nature of discontinuity offer two positional arrangements. In one case, the strips were located at the two ends (i.e., top and bottom portions coming in contact with the platens of the press) and termed non-mid-discontinuous [DN; Fig.1(b)]. In the second set of the same subclass of the discontinuous delaminating strips, the BS materials were so located that they lay near the central portion of the specimen and these were called discontinuous delamination strips at mid [DM; Fig.1(c)]. It is apt to state at this point that, in making the subclasses DN and DM, respectively, the 5-mm-wide BS were interspersed at regular dimensions of 10 mm and fur-

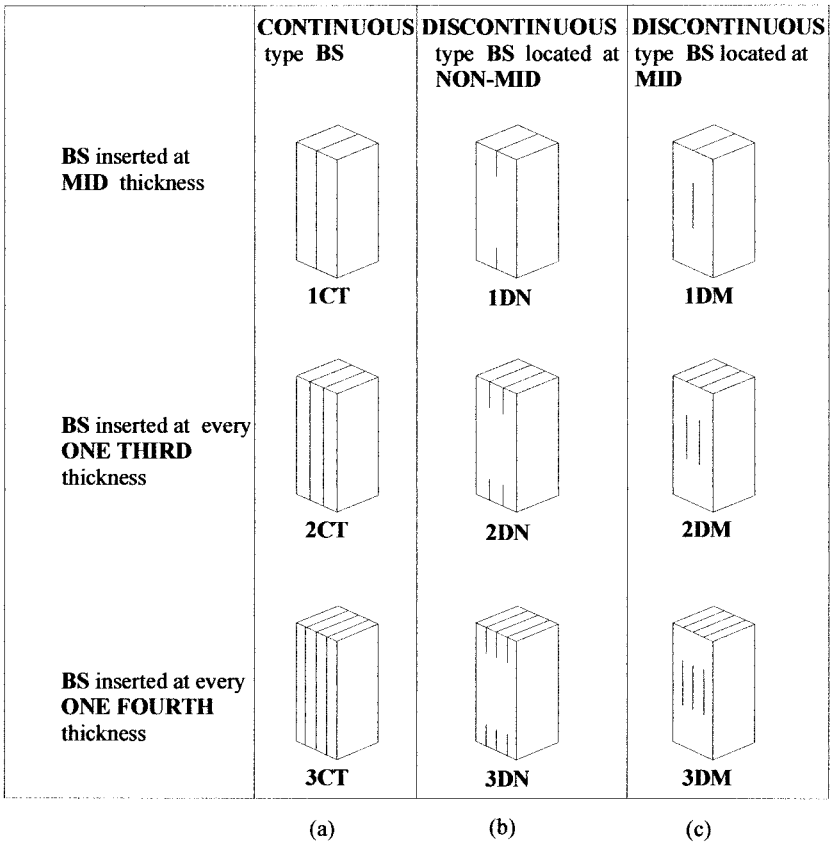

Figure 1 The different arrangements of BS inserted layers within the specimen and their codification.

ther on, while sectioning, it was ensured that the strips lay either at the central region or at the edges conforming to DM or DN classes, respectively. Thus, from a processing schedule involving both types of buffer strips (i.e., continuous and discontinuous) and their location(s) across as well as along the thickness directions, it was possible to get a combination of nine types of specimens with the codes 1CT, 1DN, 1DM; 2CT, 2DN, 2DM; and 3CT, 3DN, 3DM, respectively, allotted. These nine strip-bearing test specimens were tested in compression mode by using a Dartec machine under normal ambient conditions at a constant strain rate (possibly by using a microprocessor-operated programmed setup). The test was carried out with the stack layers parallel to the loading axis [Fig. 1(a–c)]. Specimen dimensions of 5 $\times$ 5 $\times$ 16 mm were cut using a diamond cutter. Further, for a relative type of grading, envisaged in this work, it was considered useful to have values of the plain C–E as a reference and to normalize the data derived for the other cases. The effects of inserted BS and their influence on the compressive behavior were thus looked into in the dry (i.e., unexposed) sample in the first instance.

Studies on Moisture

To gather information on the response of the same architectural detail samples to moisture, another set of similarly configured test samples were subjected to compression testing, this time following exposure to water. The specimens were exposed to an aqueous environment by immersing them in a beaker filled with water maintained at 75 $\pm$ 3°C for 1000 h. The weight of the specimen with time of exposure was monitored by using an electronic balance. The procedure involved removing the samples from the beaker, wiping out the surface water by an absorbent medium, cooling to ambient temperature, and weighing them as per ASTM–STD-D695M-91, prior to compression testing. For determining the compression properties, the procedures enumerated for dry test samples were adopted. The tests pointed to

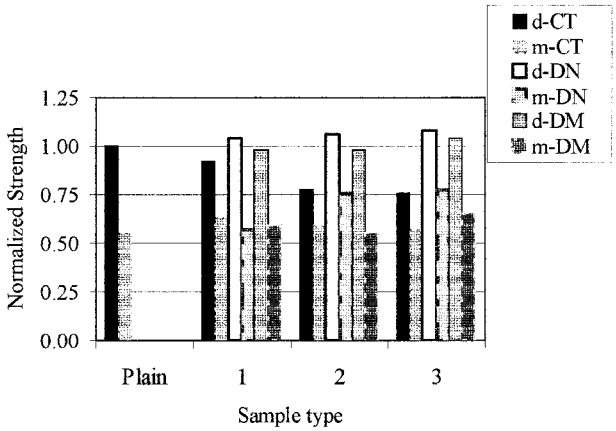

Figure 2 A plot showing the normalized compression strength values for plain C–E and all BS-bearing samples tested in both dry and water-ingressed conditions prefixed by letter d and m, respectively.

lower absorption in BS-free C–E samples and higher levels for CT type. 3CT samples showed the highest of the three BS-bearing continuous strips.

RESULTS

Variation in Strength

Figure 2 is a plot of the average compression strength data for continuous and discontinuous BS-containing samples in dry conditions and following water-ingressed conditions, denoted by prefixes the d and m, respectively. The data derived from compression experiments on at least four replicate specimens in the different architectural bearing (i.e., 1, 2, and 3 CTs, DNs, and DMs) samples are shown. Further on, the values derived on plain samples (in both dry and following immersion in water) are also included. As stated before, the values of dry C–E plain samples are used as a reference while normalizing the data for all other varieties of samples both in dry and in water-ingressed conditions.

In this article, as per the objectives, first the strength data presented in Figure 2 will be correlated with the macroscopic features for plain samples in comparison with the CTs (i.e., 1, 2, and 3 CT-type samples) in both dry and wet states. Then, this exercise will be repeated for the two discontinuous BS-inserted DN and DM samples, respectively. Thus, first considering the plain varieties, the exposed ones showed a reduction in compression strength values of about 45% compared to its dry counterpart (Fig. 2). When this exercise was repeated for the other exposed samples of the CT-type BS-bearing samples, the reduction recorded for the 1, 2, and 3 varieties varied from 37 to 43%. As regards the fractography of the dry plain samples, they showed a transverse material flow phenomenon [Fig. 3(a)], followed by a split in the longitudinal direction (i.e., along the loading axis). The transverse flow, which may be termed as lip or ear formation, is observed to be restricted to the face of the specimen coming in contact with the loading platen of the test setup. From an observation of the fracture feature displayed by this type of sample, it is noticed that there is no preference to any of the plies for the cracks to propagate during the test leading to a split. This finding implies that the plies that are weakly adhering are the probable ones for crack propagation to occur under compressive loading leading to split(s).

When the plain wet (i.e., water-immersed BS-free) samples are tested, it is observed that they exhibit a distinct inclined cracklike feature [Fig. 3(b)]. A point distinctly observed in these water-immersed and compression-tested samples is the near absence of the lip- or ear-formation [Fig. 3(b)] tendency compared to such features being exhibited explicitly by its dry counterpart described earlier [Fig. 3(a)]. To understand this singular response difference between the wet and dry conditions for the plain C–E variety, it was felt necessary to investigate the inclined crack formation feature displayed by the wet samples [Fig. 3(b)]. To achieve the objective of structure–mechanical property correlation, it was decided to examine carefully all the resin-rich areas first [Fig. 4(a,b)]. This exercise pointed out the need

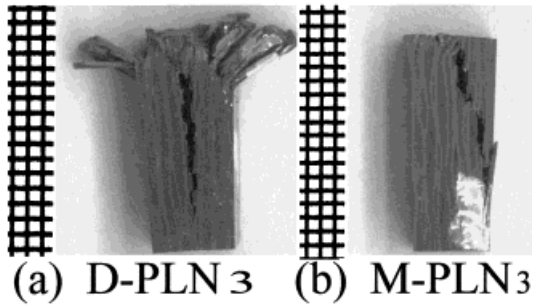

Figure 3 Photograph showing the differences in the failure pattern exhibited by the plain C–E samples when tested in (a) dry state and (b) moisture-ingressed condition.

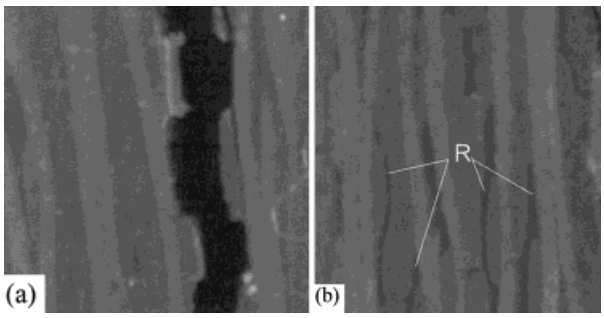

Figure 4 A magnified view of the fiber-crimp region for (a) dry samples and (b) the wet samples with the formation of microcracks. Note the proneness to microcracks in the latter.

for focusing attention to the resin-rich region [marked R in Fig. 4(b)], especially at crimp zones of the fibers running longitudinal to the specimen axis. The resin-rich regions following absorption of water molecules experience a positive dimensional change. The volumetric change worked out in the present case to be on the order of 2%. This initial dilation followed by a loss of some adsorbed water owing to reversal of the ingression trend, especially in the immediate environs of the fibers (consequent to removal of the specimen from the water bath), results in the formation of small linear-type unfilled pockets that may be termed a miniaturized local fissure for the present purpose at the fiber-matrix interface. Figure 4(b) shows the possible sites for such cracks to exist (indicated by white lines about the region marked R). The background intensity at these spots are different, owing to the creation of flaws at such regions. Both the proximity and the number of such fissures determine the ease with which the two successively posited flaws could join to pave the way for inclined cracks to form. When these microcracks join up to grow outward, then they form a separate crack ending up at the sides of the test specimen (as in the right-side-posited inclined split) in Figure 3(b). On the other hand, if the microcrack is posited such that an inward growth is favored, the inclined crack forms and extends until such a time as it meets the main crack, along which finally a split section is seen [top of Fig. 3(b)]. Thus, the locations of these microcracks, their orientation, and further growth can be brought in to explain first the differing macroscopic features among wet samples and then between wet and dry plain C–E samples. The sequential events of this nature also explains the lesser occurrence of lips at the end of the specimen in contact with the platen in water-ingressed samples compared to the dry ones. In the dry samples, considerable lateral material flow occurred [Fig. 3(a)], resisting the applied load before a ply could favor a split to be effected into the entire length of the test coupons. The split occurs where the bond between plies is weak. This way it is possible to establish the higher strength and lip formation for the dry compared to the wet variety for the BS-free test specimens.

Also observed from the data in Figure 2 is that in the dry case, the plain sample (i.e., without inserted BS) shows the maximum compression strength compared to any of the three (i.e., 1, 2, and 3) CT-type specimens. Also obvious from the graph [Fig. 2] is the fact that load-bearing ability diminishes with increased numbers of continuous BS content in the test coupons. The decrement generally ranges from 8% for 1CT to 24% for 3CT, whereas 2CT showed an intermediate value of 22% [Fig. 2]. This decreasing strength with an increase in the BS layer is understandable because each PTFE-coated strip insertion favors a greater level of occurrence of delamination at the strip/C–E interface, thereby reducing the maximum load sustainable by the test coupon. Supporting this proposition of delamination at the interface is the microscopic observation made in dry 1, 2, and 3 BS layer containing CT-type samples [Fig. 5(a–c)]. The photographs in Figure 5 show a clear split along the BS-inserted plies. As the ease of split is favored by the presence of less adhering strips, the outward material flow representing the resistance offered by the system to compression is considerably decreased. Consequently the ear formation tendency is almost absent. Thus, the one-to-one correlation between strength data and macroscopy seen in the dry state for plain samples is repeated in this architectural arrangement.

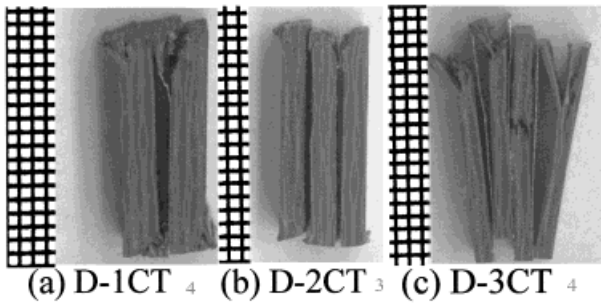

Figure 5 Photograph showing the longitudinal split formation in dry state for (a) 1CT, (b) 2CT, and (c) 3CT varieties.

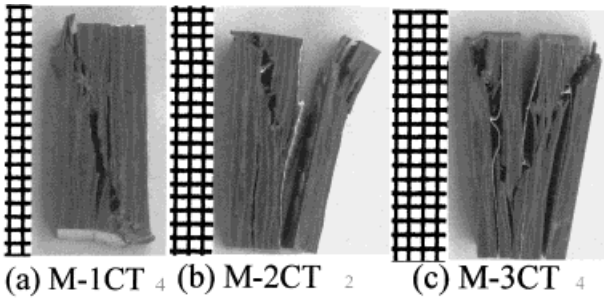

Figure 6 Picture showing the failure mode in moisture-exposed samples belonging to (a) 1CT, (b) 2CT, and (c) 3CT varieties.

To explain the lesser drop in strength of CT-type samples than that of plain-type samples following water ingression, it is worthwhile to first recall that water ingress increases with the number of BS insertions.[11] This enhanced level of water absorption over that seen in plain type (owing to interfaces of strip/C–E region acting as temporary sinks as stated earlier) can lead to a situation where the water acts as a medium filling the voids and thereupon restores a continuity within the system for the load transfer from the matrix to reinforcement to take place. In addition to this, the expansion of resinous medium facilitates good resin-to-resin contact through the sievelike pores of the PTFE-coated fabric to be established. Consequently, paths for crack propagation other than the interface region involving the BS strip are activated. The resulting situation is that seen in Figure 6, where both conventional vertical split and inclined cracks form simultaneously. Thus, Figure 6(a) shows a transverse crack joining in a longitudinal crack. Figure 6(b) shows two major cracks to which other minor cracks join in. Finally, in Figure 6(c) three well-formed cracks to which inclined cracks joined can be seen. Of these, the last one (i.e., 3CT varieties) having the highest water absorption (therefore, prone to plasticizing to a considerable extent) exhibits the path changes for the crack to grow. This point is emphasized in Figure 6(c). The plasticizing of the epoxy matrix by the absorbed moisture has a profound countering effect as for the way the delamination occurs, especially where the strip-bearing region in the BS-containing samples are concerned [Fig. 6(c)]. The change in the progression of the crack paths reflects the prolonging of the path of the crack in the water-immersed BS-bearing sample. This slow progress is related to greater resistance offered by the material to compressive deformation. This way, the less spectacular drop seen in CT-type water-immersed samples can be explained by the use of microscopy.

The dry varieties show longitudinal splits irrespective of whether the laminate is with or without the BS material. The difference in macroscopy as far as the BS-free and BS-containing samples are concerned arises on two fronts: (i) the lip formation, and (ii) the ease of separation (especially in continuous BS-bearing cases). When the aqueous media are present, a twofold influence takes place. First, greater water absorption occurs with an increase in BS material (because a path of easy diffusion is provided by the strips' increases with the number of BS layers inserted in the sample). Then, the water reaches the interior of the samples because of greater ingress, which is again a function of the BS-interface area that increases with a higher number of BS insertions. This results in swelling and microcrack formation favoring inclined crack propagation, especially at crimps discussed earlier.

Having considered the continuous buffer strip inserted cases, what follows is a discussion of discontinuous DN and DM types where, as stated earlier, the strips are posited closer to the ends of the coupons and adjoining to the place where the platens come in contact with the test sample and at the center of the test coupon, respectively, as discussed earlier. Thus, taking the DN case first, in the dry state they showed compressive strength value, which displays a stepwise steady increase of 4, 6, and 8%, respectively, for the three varieties [i.e., 1, 2, and 3DN (Fig. 2)]. Also, the 2DN and 3DN varieties in water-immersed cases show higher strength than the corresponding 2CT and 3CT samples. This is explainable when it is recalled that the region between adjoining strip locations are the regions where only C–E materials are present and where crack detoured noted earlier for plain samples can occur. This way the material resists applied load better in DN variety than in CT cases where the path for easy delamination is readily provided by the C–E/BS interface. Also noted is the fact that when the moisture-exposed samples of the DN type are considered, they too show a pattern similar to their dry counterparts described before; namely, there is a general increase in the compression strength with an increase in the number of buffer strip insertions made (Fig. 2). However, if instead of comparing the dry and wet varieties separately, an attempt is made to see how the change in

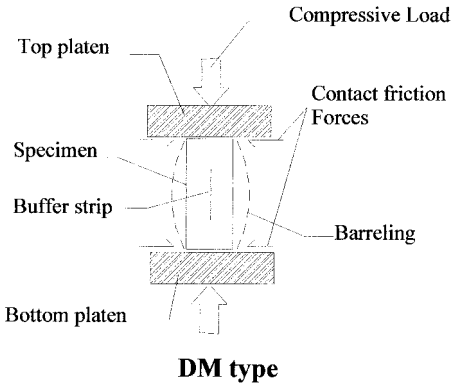

Figure 7 A schematic figure showing the arrangement in compression and the resultant barreling in DM type.

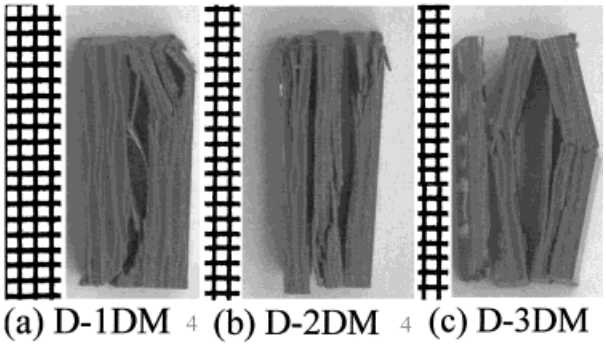

Figure 8 Photograph showing the wider gap at the central region bearing the BS strip and barreling tendency for (a) 1DM, (b) 2DM, and (c) 3DM tested in the dry conditions.

strength values for any given type occurs following exposure, it is noticed that the maximum drop occurs for the plain variety, whereas BS inserted 1, 2, and 3DN samples show a lesser decrement following exposure than the corresponding values derived in the dry state. Further, DN samples generally show greater strength than DM type in water-ingressed cases. These clearly show, all things being the same, that the continuity or otherwise of the strips and hence their location has a greater bearing in wet conditions. In other words, the strength loss introduced by the absorbed moisture in the matrix for the BS-free type is in a way countered by the changed structural situation prevailing because of BS insertion plus water adsorption at a less adhering weakly bonded interfacial region involving BS strip/C–E interface.

Figure 7 shows schematically the positioning of the buffer strip vis-à-vis the platen of the press. The DM type favoring a barreling is illustrated in the line drawing. This kind of bulging is assisted by transverse tensile stresses along the width face, which in conjunction with the presence of BS strip at such regions and absence of the same at the top and bottom contact faces, makes the barreling a likely event. Should this be the actual situation, then it should favor a debonding process to be initiated which ideally begins at the center of the DM specimen, owing to the presence of the BS at that region, and proceeds toward the two edges. In such a situation, the width of the debonded central zone should be larger than that experienced by the locations on the specimen that are either closer to the top or bottom platen in the compression test setup. That such a situation actually prevails in the test coupon is evidenced in Figure 8(a). That this is the case, in not only the single-layer inserted samples, but also in 2 and 3 layer inserted ones, is unambiguously demonstrated in Figures 8(b) and 8(c), respectively. Thus, for instance, in Figure 8(a), the debonding in 1DM is in the central zone and its incomplete progression toward the top end (top platen) is clearly pictured. Consequently, the strength values of these DM varieties should be lower than that seen in DN where [as shown in Fig. 9(a–c)] a clear tendency for the crack to initiate at the top platen and progress downward where the strip-free material is present is often witnessed. Thus, macroscopy aids ably the strength data analysis in this case of the DN and DM variety tested in the dry state also.

The DM and DN samples in water-immersed conditions show the inclined crack feature and its joining of the main one [Figs. 10(a) and 10(b),

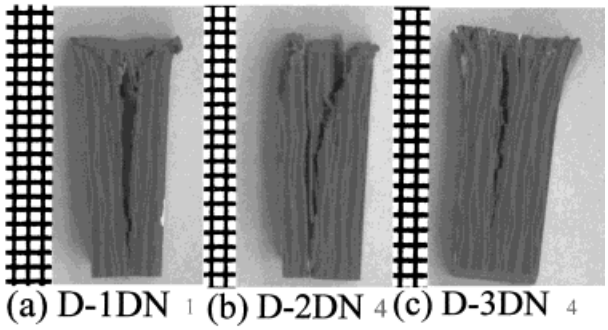

Figure 9 Photograph showing the formation of the Y-fork shaped failure pattern initiated by the presence of the BS strip at the contact faces of the specimen in (a) 1DN, (b) 2DN, and (c) 3DN samples tested in the dry conditions. Note the absence of the barreling effect earlier seen in the DM type of samples.

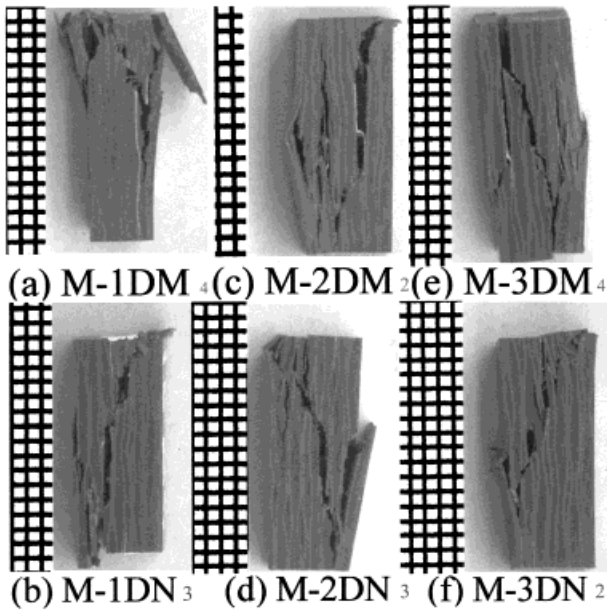

Figure 10 Pictures showing the predominant inclined fracture mode of the moisture-exposed samples irrespective of the BS arrangement in the discontinuous type samples (a) 1DM, (b) 1DN, (c) 2DM, (d) 2DN, (e) 3DM, and (f) 3DN.

respectively]. Alternately, a stepwise shift of the crack is recorded [Figs. 10(c–f)], which clearly demonstrates this expected admixtured feature of plain and CT-type samples discussed earlier in these discontinuously distributed BS layers. Thus, the macroscopy can also be correlated with the architecture, keeping the test conditions the same.

Trends in Modulus Variations

Figure 11 shows the variation in compression moduli for various architectures of the samples. As is to be expected, the changes here [Fig. 11] are less discernible than the strength data [Fig. 2] presented and discussed earlier. Here again both dry and moisture-exposed data are represented and a comparison with the plain samples in their dry state, as referred earlier. It is observed that the compressive modulus for the plain as well as the CT varieties shows no difference in the modulus values when tested in dry conditions. However, on exposure to moisture, the patterns are slightly different. The plain samples show a noticeable reduction in the modulus value, whereas the reductions for 1, 2, and 3CT are smaller.

As regards the DN varieties, all three varieties (i.e., 1, 2, and 3DN) in the dry state display modulus values, which are higher than the plain values. However, when the same DN samples are exposed to water by immersing the test samples in the liquid medium, the changes in values are less markedly noticed [Fig. 11]. Addressing the DM variety, they too show a trend similar to that seen earlier on for DN variety. In other words, the moduli variation for the dry DM and DN cases is not too distinct. The modulus values are not that sensitive to the position occupied by these discontinuous strips in the test coupon.

CONCLUSION

The foregoing analysis point to the following conclusions.

Continuous strip-bearing samples in the dry state show a decrease in strength with increased insertions of BS layers. This is ascribed to the debonding occurring at the BS-inserted region and supported by one-, two-, and three-layer separations during macroscopic examinations of the 1, 2, and 3CT samples.

Water-ingressed CT-bearing samples show a small rise in strength compared to water-ingressed plain samples. The resin expansion and plasticizing of the resinous region make the crack propagation a tortuous one. This argument is well supported by macroscopy. Further, it was shown that the resin-rich crimp area plays a significant role in that it determines whether the propagating crack joins a main one inside the test coupon or emerges at the side of the test sample. Support for this could be obtained through microscopy

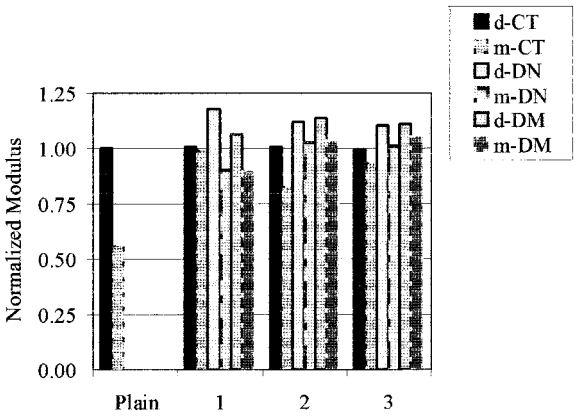

Figure 11 A plot showing the normalized compression modulus values for plain C–E and all BS-bearing samples tested in both dry and water-ingressed conditions prefixed by letter d and m, respectively.

where for the dry state it had a vertical split with considerable lateral flow, whereas the water-exposed sample showed inclined cracks for the three BS-bearing categories.

Discontinuous samples show less readiness to splitting, especially for the DN type compared to the DM type. Of the two discontinuous types, the DM type showed a kind of barreling effect.

Water ingression in these discontinuous samples makes the crack shift its path significantly and this shift is aided by the absence of strip-bearing regions inside the test coupons, owing to specific architectures adopted during fabrication.

The first author thanks the members of the polymer composite lab for the assistance rendered at various stages of the work. He also thanks the chairman Professor D. H. Sastry for the use of the facilities and for the interest shown during the various stages of the work. The second author expresses gratefulness for the extreme help provided by Mr. Shanthkumar and Mr. Satyananda of HAL, ALH-composite shop, and Mr. S. Sasidhara of the Processing Lab at the Dept. of Metallurgy in IISc, without which this work would have been incomplete. He also appreciates the cooperation of his colleagues at RCMA (H) Bangalore and his lab mates in the polymer composites lab for support. All the authors thank the Director of ADE for showing keen interest in this work.

REFERENCES

1. Yasunobu, H.; Hiroyuki, H.; Jang-Kyo, K. Compos Sci Technol 1998, 58, 91–104.
2. Poe, C. C, Jr.; Kennedy, J. M. J Compos Mater Suppl 1980, 14, 57–70.
3. Tai, N. H.; Yip, M. C.; Lin, J. L. Compos Sci Technol 1998, 58, 1–8.
4. Kinloch, A. J.; Shaw, S. J.; Tod, D. A.; Hunston, D. L. Polymer 1983, 24, 1341–1354.
5. Ghasemi-Nejhad, M. N.; Parvizi-Majidi, A. Composites 1990, 21, 155.
6. Kishore;Khan, B.; Viswanath, B. Compos Interface to appear.
7. Hahn, H. T.; Hwang, D. G. ASTM STP787; Annu Book ASTM Stand 1982, 247–273.
8. Simitises, G. J.; Sallam, S.; Yin, W. L. AIAA J 1985, 9, 1437–1445.
9. Mustafa, A.; Wiliam, M. B. Compos Struct 1998, 42, 1–12.
10. Freitas, M. D.; Reis, L. Compos Struct 1998, 42, 365–373.
11. Kishore; Khan, B.; Viswanath, B. J Reinforced Plast Compos, to appear.